논문번호 05-02-09

Ultrashort Optical Pulse Generation at 10 GHz by Pulse Compression of Actively Mode-Locked Fiber Laser Output

능동 모드잠금 광섬유 레이저 출력의 펄스 압축에 의한 10 GHz 극초단 광 펄스 발생

Dongsun Seo* and Andrew M. Weiner**
徐東善*, 앤드류 와이너**

Abstract

We report 400 femto-second highly stable, nearly transform-limited, pulse generation at 10 GHz in 1540 ~ 1550 nm wavelength region by adiabatic soliton pulse compression of an actively mode-locked fiber ring laser output. Without using any supermode selection device, supermode beating noise has been suppressed below -123 dB/Hz, resulting less than 100 femto-second timing jitters at the noise band of 1 kHz ~ 100 MHz.

요 약

모드잠금 고리형 광섬유 레이저 출력의 단열 쏠리톤 펄스압축에 의해 1545 ~ 1550 nm 파장영역에서 400 펨토초의 안정성이 뛰어난 변환제한급의 10 GHz의 광 펄스를 발생시켰다. 특별한 슈퍼모드 선택소자를 사용하지 않고도 -123 dB/Hz 이하의 슈퍼모드 비팅 잡음 억제에 의해 1 kHz ~ 100 MHz의 잡음대역에서 100 펨토초 미만의 낮은 시간 지터를 얻었다.

Key Words: Optical Pulses, Mode-Locking, Pulse Compression, Optical Communications.

I. Introduction

Highly stable, high repetition-rate femto-second sources are very attractive for a number of applications including ultrahigh speed optical communication, optical sampling, and spectroscopy. One of typical method to generate such femtosecond pulses is to compress an actively mode-locked fiber ring laser output with a few pico-seconds (ps) of pulse width ([1],[2]). However, actively mode-locked fiber ring laser outputs may show large pulse-to-pulse timing jitter approaching to an order of picosecond ([3]). This relatively large timing jitter is induced by multiple supermode excitation in a relatively long fiber ring laser cavity ([3]). To suppress this supermode excitation, a Fabry-Perot (FP) etalon filter with a free spectral range (FSR) at exactly the mode-locked laser repetition rate has been inserted inside the laser cavity ([4],5]). This requirement of strict matching between the repetition rate and FSR results that the output pulse

* 明知大學校 電子工學科
(Dept. of Electronics, Myongji Univerity)
** 퍼듀大學校 電氣工學科
(Dept. of Electrical Engineering, Purdue Univerity, USA.)

※ T his work was supported by Korea Research Foundation Grant (KRF-2004-042- D00140)
接受日:2005年 8月 31日, 修正完了日:2005年 12月 14日

width critically depends on the repetition rate of which flexibility is limited within 10 kHz. Here, we discuss highly stable, wavelength tunable, femto-second pulse generation at 10 GHz by adiabatic pulse compression of an actively mode-locked fiber ring laser without any supermode selection device.

II. Acively Mode-Locked Fiber Ring Laser

Our experimental setup is shown in Fig. 1. The actively mode-locked fiber ring laser has a common configuration, which consists of a polarization controller (PC), linear polarizer (LP), intensity modulator, isolator, erbium-doped fiber (EDF), and wavelength tunable band pass filter (BPF). All of the laser loop, except between the LP and modulator, is made up of standard non-PM fibers and devices. The 12-m long EDF is both backward and forward pumped for higher gain by laser diodes at 980 nm. The total cavity length was 21 m and the total pumping power level was 450 mW. For cavity length stabilization, the phases of the modulator drive signal and laser output detected by a 23 GHz photo-detector are compared at a radio frequency mixer and the error signal amplified by a high voltage (HV) amplifier is fed back to the cavity through the piezoelectric translator (PZT) to stretch the EDF ([2]).

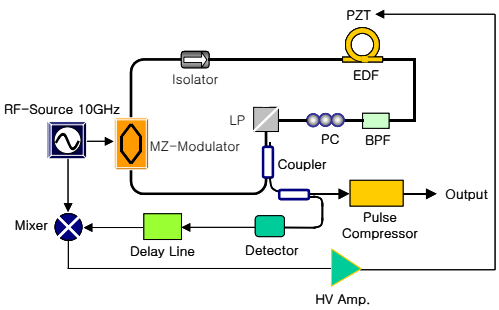

Fig. 1. Experiment schematic.

In a strongly pumped mode-locked laser, a soliton compression can be achieved inside the laser cavity ([1]). This indicates the pulse shape depends on its pick-up position inside the cavity ([6]). Generally the output shows blue chirp which can be easily compensated by a normal single mode fiber (SMF). Our laser output showed 3.7 ps of the pulse width (assuming Gaussian shape) and 1.3 nm of the spectral width, resulting in the time-band width product (TBP) of 0.62. The large TBP indicated that the output pulses were chirped. By compensating the chirp using a 115-m length of an SMF, 3.7 ps of direct output pulses could be reduced to 2.7 ps as shown in Fig. 2, resulting in the TBP reduction from 0.62 to 0.45, which was slightly greater than the transform-limited value of 0.414.

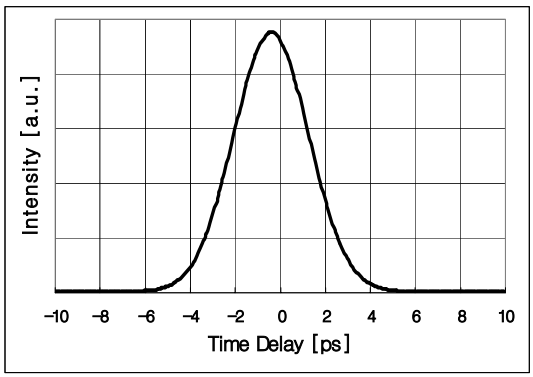

Fig. 2. Autocorrelation traces of the chirp-compensated mode-locked output.

Fig. 3 shows the corresponding optical spectrum with 1.3-nm width. We can clearly see the spikes with 0.08-nm spacing in the optical spectrum, indicating 10 GHz optical pulses. The extinction ratio between the peak and valley was greater than 20 dB, indicating stable mode excitation leading to the great suppression of the supermode beating noise (*i.e.*, pulse-to-pulse timing jitter).

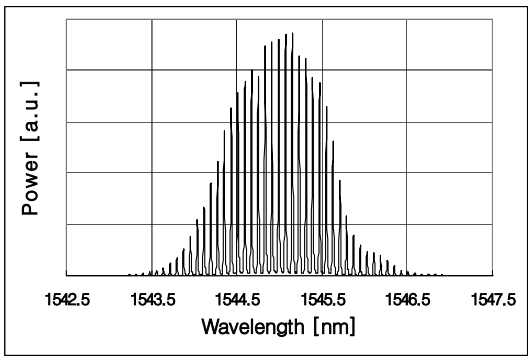

Fig. 3. Corresponding optical spectra to Fig. 2.

To confirm the supermode beating noise suppression, we simultaneously measured the radio frequency (rf) spectrum around the pulse repetition frequency at 10 GHz by a fast photo-detector coupled with an rf spectrum analyzer, as shown in Fig. 4. The supermode beating noise peaks with 9.4 MHz spacing could be barely observed and compressed up to 83 dB @ 10 kHz resolution bandwidth, corresponding to -123 dB/Hz noise suppression. The measured timing jitter based on the noise spectrum ([7]) at the noise band of 1 KHz ~ 100 MHz was ~100 femto-seconds (fs). We believe that the inherent stability of the output pulses comes from the relatively short cavity length of 21 m and the high pumping level at 450 mW.

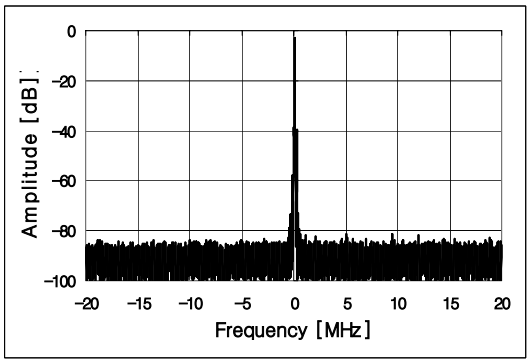

Fig. 4. Noise spectrum around 10 GHz.

Next, we tuned the BPF inside the laser cavity shown in Fig. 1, and produced nearly transform limited, 3-ps Gaussian pulses over 1543 ~ 1565 nm. There was no noticeable change in the output pulse stability over the tuning range.

III. Pulse Compression by a DDF

One of common methods to achieve pulse compression without pedestal generation is an adiabatic soliton compression based on dispersion decreasing fiber (DDF). If we inject a fundamental soliton pulse into a DDF, the pulse would like to keep fundamental soliton by reducing its width. Let's recall the peak power P_{pk} of the fundamental soliton at a given fiber with a dispersion D,

$$P_{pk} = 0.776[\frac{\lambda^3}{\pi^2 c n_2}][\frac{\mathrm{A}_{eff} D}{\tau_p{}^2}] \quad (1)$$

Where, n_2 , A_{eff}, and τ_p represent nonlinear coefficient, effective fiber core area, and pulse width, respectively. When the soliton pulse passes through a lossless DDF, the pulse energy E will not be changed,

$$E = P_{pk} * \tau_p \propto [\frac{\mathrm{A}_{eff} D}{\tau_p{}^2}] * \tau_p = const \quad (2)$$

This indicates that the pulse width should decrease as the dispersion decreases. From the relationship, we get an achievable pulse compression ratio R by passing through the DDF.

$$R(z) = \frac{\tau_o(0)}{\tau_p(z)} = \frac{D_o(0)}{D_p(z)} \quad (3)$$

where the subscripts o and p indicate the initial and final values of a given variable. An ideal dispersion profile is known to be an exponentially decaying profile. However, it requires longer fiber length to

avoid pulse pedestal generation. In addition to that the fiber loss also requires to modify the profile. In practice, it is close to a linear profile. In any case, to achieve larger compression, the input dispersion should be as large as possible, while the output should be as low as possible. But, a larger dispersion value requires a higher power to form fundamental soliton, which may not be possible in current state-of-art technology of an optical amplifier. Too small dispersion may give a negative dispersion value at the edge of the interested wavelength bandwidth. Generally the dispersion decreases from 10 to 1 ps/nm/km, allowing the compression ratio of 10. Here we used a Pritel soliton compressor which included a high power erbium-dopped fiber amplifier (EDFA) and a 2-km length DDF with 2 dB loss. We passed the mode-locked output through the DDF for adiabatic soliton compression.

Figs. 5 and 6 show the autocorrelation trace and optical spectrum of the compressed pulses. The pulse width was compressed from 2.7 ps (Gaussian shape) to 0.65 ps ($sech^2$ shape), while the spectral width was broadened from 1.3 nm to 4 nm. This results in the TBP of 0.33, which is very close to the transform-limited value of 0.315. No pedestal was observed in the compressed pulses and the optical spectrum shows clear peaks with 0.08 nm (10 GHz) spacing. The achieved pulse compression ratio of 4 was slightly lower than the ideal value of 6.5, which was given by the DDF supplier (Pritel). We may imagine a couple of possible reasons; 1) the compression ratio was sacrificed to minimize pulse pedestal generation (as shown in Fig. 5, the pedestal power was less than 1%), and 2) the input pulses might not be perfectly transform-limited. Note also that, since the pulse compressor is a passive device, the compressed pulses have the similar supermode beating noise suppression and pulse timing jitter as the input pulses.

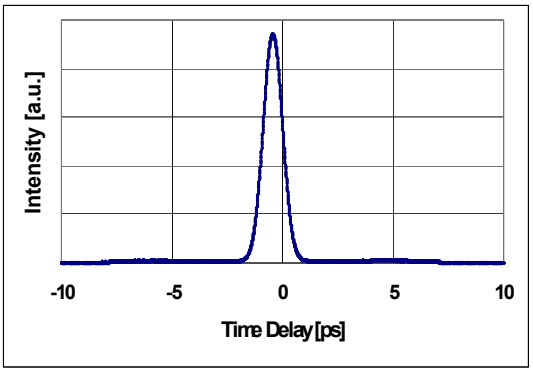

Fig. 5. Autocorrelation trace of the compressed pulses.

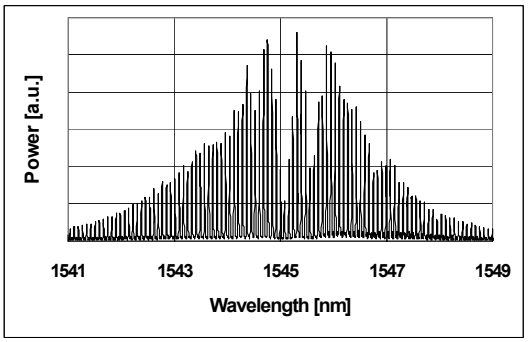

Fig. 6. Corresponding optical spectrum of Fig. 4.

Next we tuned the output wavelength by adjusting the BPF in Fig 1 and successfully generated highly stable femto-second pulses in the 1543 ~ 1563 nm wavelength region, as shown in Fig. 7. The TBP values stay at 0.3 ~ 0.4, showing nearly transform-limited $sech^2$-shaped pulses. We also observed that slight variations in the pulse widths of the mode-locked laser output did not change the compressed pulse characteristics noticeably. However, too broad compressor input pulses enhanced pedestals in the compressed output.

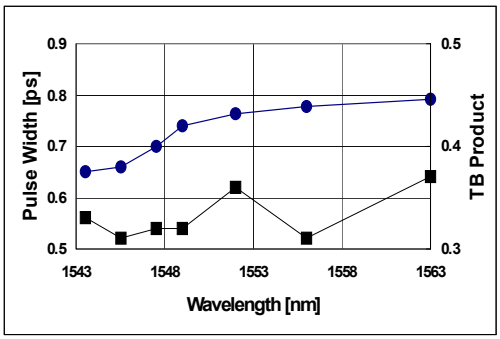

Fig. 7. Output pulse widths (circles) and time-bandwidth products (rectangles) at several wavelengths.

IV. Pulse Compression by a Modified DDF

According to the data given by the DDF vendor (Pritel), the dispersion of our DDF decreases from 10 to 1.5 ps/nm/km at 1545 nm, resulting in the pulse compression ratio of 6.5 even at an ideal case. To achieve greater pulse compression ratio, we need to increase the initial dispersion value D_o and/or to decrease the final value D_p of the DDF. This means that, by combining a high dispersion fiber at the front and/or a low dispersion fiber at the end of the DDF as shown schematically in Fig. 8, we can increase effectively the input-to-output dispersion ratio to get better pulse suppression ratio.

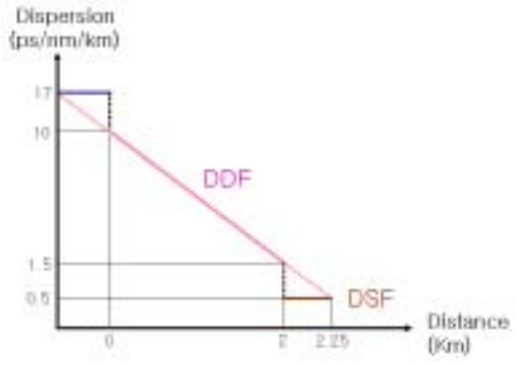

Fig. 8. Attachment of an external fibers to modify the DDF profile to achieve better pulse compression.

As we discussed before, the former may not be desirable since it requires higher power to form a fundamental soliton at the input. The latter has been applied in this experiment by connecting a dispersion shifted fiber (DSF) with zero dispersion at 1541.2 nm at the end of the Pritel DDF. The length of the DSF has been determined by a try-and-error method. A shorter fiber gives shorter spectral width even if the temporal pulse shape shows lower pedestals. A longer fiber provides more nonlinearity, giving broader spectral width. However it gives larger pedestals, requiring a band-pass filter to eliminate them.

As a compromising configuration, we chose an 83-m length of DSF fiber. Fig. 9 shows optical spectra (a) and autocorrelation traces (b) of the fiber compressor output at various DDF input pulse power levels (the input signal power was increased from top to bottom). The measured spectral and pulse widths from top to bottom were; 5.5 nm and 360 fs at 105 mW (top), 4.8 nm and 349 fs at 110 mW (second from top), 4.3 nm and 335 fs at 115 mW A (middle), 3.8 nm and 320 fs at 125 mW (second from bottom), and 10 nm and 266 fs at 160 mW (bottom), respectively. Note that, at the maximum power level of 160 mW, the fiber compressor output started to show super-continuum broadening. The 266 fs pulse may be cleaned by passing a pulse cleaner, such as a dispersion unbalanced nonlinear loop mirror. Fig. 9(b) shows clearly that, the pulse width decrease as the pumping power increases at the cost of the pedestal power increase. Even at 105 mW, the pulse shows noticeable pedestals. To minimize the pedestal power, we sacrificed the pulse width a little bit and operated at 95 mW, where the output showed 380 fs with 6-nm spectral width, resulting in the TBP of 0.28. The TBP indicates that the pulse shape is neither Gaussian nor sech^2. Typical optical spectra (a) and autocorrelation traces (b) before (solid lines) and after (dotted lines) pulse compression at 95 mW are shown in Fig. 10. The figures show that the spectral width increases from 1.3 nm to 6 nm, while

the pulse width decreases from 2.7 ps to 0.38 ps, respectively.

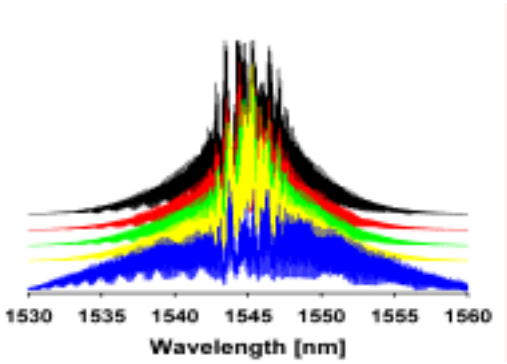

(a)

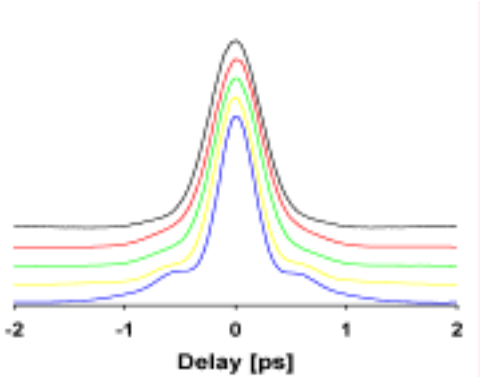

(b)

Fig. 9. Optical spectra (a) and autocorrelation measurements (b) of the compressed pulses by the modified DDF at various DDF input power levels; 105 mW (top), 110 mW (second from top), 115 mW A (middle), 125 mW (second from bottom), and 160 mW (bottom).

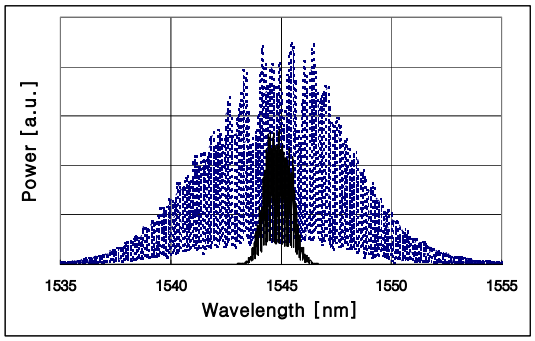

(a)

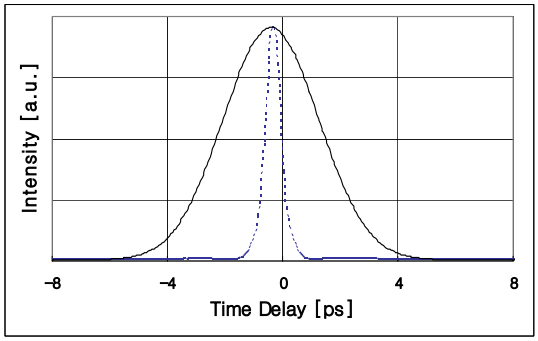

(b)

Fig. 10. Optical spectra (a) and autocorrelation traces (b) before (solid lines) and after (dotted lines) the optimum pulse compression.

Finally we tuned the wavelength and could obtain less than 400 fs pulses for the wavelength range from 1540 nm to 1550 nm, even if slight increment of the pulse pedestal power was observed. To confirm the stability of the output pulse train, we compared the intensity auto- and cross-correlation (between the neighbourhood pulses) traces at the DDF input power of 125 mW. The traces showed a negligible difference between the auto- and cross-correlation widths; 348 fs and 353 fs, respectively. From this information we can simply obtain the high frequency (greater than 2 GHz) pulse-to-pulse timing jitter of 60 fs ([8]).

V. Conclusion

We have achieved 400 femto-second highly stable, nearly transform-limited, pulse generation at 10 GHz in the 1540 ~ 1550 nm wavelength region by adiabatic soliton pulse compression of actively mode-locked fiber ring laser with no supermode selection device. The measurement of the radio frequency spectrum by a fast detector showed supermode noise suppression greater than -123 dBc/Hz and the pulse-to-pulse timing jitter less than 100 femto-seconds at the noise band of 1 kHz ~ 100 MHz. The comparison between auto- and cross-correlation widths showed negligible difference, confirming very small pulse timing jitter at high frequency region, too. We expect the pulse source can play a critical role in many applications, such as ultrafast optical communications, optical sampling, optical code-division multiple access, etc.

References

[1] T.F. Carruthers and I.N. Duling III, "10-GHz, 1.3-ps erbium fiber laser employing soliton pulse shortening", Opt. Lett., vol. 21, no. 23, pp. 1927-1929, Dec. 1996.

[2] J. Li, P.A. Andrekson, and B. Bakhshi, "Direct generation of subpicosecond chirp-free pulses at 10 GHz from a nonpolarization maintaining actively mode-locked fiber ring laser", IEEE Photon. Technol. Lett., vol. 12, no. 9, pp. 1150-1152, Sept. 2000.

[3] A.M. Braun, V.B. Khalfin, M.H. Kwakernaak, W.F. Reichert, L.A. DiMarco, Z.A. Shellenbarger, C.M. DePriest, T. Yilmaz, P.J. Delfyett Jr., J.H. Abeles, "Universality of mode-locked jitter performance", IEEE Photon. Technol. Lett., vol. 14, no. 8, pp. 1058-1060, Aug. 1998.

[4] J.S. Wey, J. Goldhar, and G.L. Burdge, "Active harmonic modelocking of an Erbium fiber laser with intracavity Fabry-Perot filters", J. Lightwave Technol., vol. 15, no. 7, pp. 1171-1180, Jul. 1997.

[5] C.M. DePriest, T. Yilmaz, P.J. Delfyett Jr., S. Etemad, A. Braun, and J. Abeless, "Ultralow noise and supermodesuppression in an actively mode-locked external-cavity semiconductor diode ring laser", Opt. Lett., vol. 27, no. 9, pp. 719-721, May 2002.

[6] K. Tamura, L.E. Nelson, H.A. Haus, and E.P. Ippen, "Soliton versus nonsoliton operation of fiber ring lasers", Appl. Phys. Lett., vol. 64, no. 2, Jan. 1994.

[7] A.J. Taylor, J.M. Wiesenfeld, G. Eisenstein, and R.S. Tucker, "Timing jitter in mode-locked and gain-switched InGaAsP injection lasers", Appl. Phys. Lett., vol. 49, no. 12, pp. 681-683, Sept. 1986.

[8] L.A. Jiang, S.T.Wong, M.E. Grein, E.P. Ippen, and H.A. Haus, "Measuring timing jitter with optical cross correlations", IEEE J. Quantum Electron., vol. 38, no. 8, pp. 1047-1052, Aug. 2002.

저 자 소 개

서 동 선 (정회원)

1958년 2월 28일생. 1980년 2월: 연세대학교 전자공학과(공학사). 1985년 8월: 연세대학교 대학원 전자공학과(석사).

1989년 12월: University of New Mexico 전기공학과(박사). 1994년 7월 - 1995년 7월: 호주 멜버룬 대학 광자공학연구실 객원연구원. 2002년 2월 - 2004년 2월: 미국 퍼듀대학교 전지공학과 객원교수. 1990년 3월 - 현재: 명지대학교 전자공학과 교수.

<주관심분야> 광부호분할다중통신, 극초단 광펄스, 광통신, 광자기술, 광계측, 등임.

Andrew M. Weiner

1979년: MIT 응용물리학과(학사).
1981년월: MIT 대학원 응용물리학과(석사).
1984년: MIT 대학원 응용물리학과(박사).
1984년 - 1992년: Bellcore 연구원 및 매니저.
1992년 - 현재: 퍼듀대학교 전기공학과 교수.
<주관심분야> 극초단펄스 형상제어, 극초단펄스 스펙트로스코피, 광부호분할다중통신, 밀리메터파 광자기술, 광통신, 등임.